Lab on a Chip

RSC Publishing

CRITICAL REVIEW

View Article Online
View Journal | View Issue

Cite this: *Lab Chip*, 2013, **13**, 3481

Chip-based liver equivalents for toxicity testing – organotypicalness *versus* cost-efficient high throughput

Eva-Maria Materne,*[a] Alexander G. Tonevitsky[b] and Uwe Marx[a]

Received 20th February 2013,
Accepted 17th April 2013

DOI: 10.1039/c3lc50240f

www.rsc.org/loc

Drug-induced liver toxicity dominates the reasons for pharmaceutical product ban, withdrawal or non-approval since the thalidomide disaster in the late-1950s. Hopes to finally solve the liver toxicity test dilemma have recently risen to a historic level based on the latest progress in human microfluidic tissue culture devices. Chip-based human liver equivalents are envisaged to identify liver toxic agents regularly undiscovered by current test procedures at industrial throughput. In this review, we focus on advanced microfluidic microscale liver equivalents, appraising them against the level of architectural and, consequently, functional identity with their human counterpart *in vivo*. We emphasise the inherent relationship between human liver architecture and its drug-induced injury. Furthermore, we plot the current socio-economic drug development environment against the possible value such systems may add. Finally, we try to sketch a forecast for translational innovations in the field.

Introduction

According to the United Nations, more than 624 pharmaceutical products have been banned, withdrawn, severely restricted, or not approved by governments since the late-1950s.[1,2] Drug-induced liver injury (DILI) is one of the most prominent reasons. This underlines the exposure of the human liver to toxic agents against the background of its gatekeeping drug metabolism and detoxification duty in man. Industrially established high throughput hepatocyte test assays in static 2D or 3D tissue culture are limited to the assessment of perturbations in pathways of toxicity (PoTs) only at the molecular, organelle and cellular levels of hepatocytes. Predictiveness of animal testing suffers from the phylogenetic distances between animals and humans. New chemical entities (NCEs) fail (46%) in subsequent clinical studies in humans due to toxicity.[3] The outstanding importance that liver toxicity has for regulatory bodies is reflected in the following quote from the US Food and Drug Administration (FDA): ''The presence of even a single case of severe liver injury resulting from treatment in the premarketing clinical trials database is a signal of a high level of hepatotoxic risk.''[4] Therefore, the industry is in dire need of model systems for drug candidate testing that are of significantly better predictive value for drug-induced liver injury in humans. A much better match of *in vitro* liver models to human *in vivo* biology is urgently required to predict the mode-of-action (MoA) at liver organ level, and to eventually trace the entire adverse outcome pathway (AOP)[5] of an unknown toxic agent from the molecular initiating event up to the individual human organism. The National Research Council in the USA has put forward their *Toxicity Testing in the 21st Century* vision,[6] which has been backed by all the relevant governmental institutes,[7] to transform environmental health protection.[8] The US Environmental Protection Agency's ToxCast research programme, with a commitment to transparency and the public release of all data, was launched in 2007.[9] In the EU, driven by animal protection movement spirit and regulatory pressure, an impressive number of scientific initiatives in this regard have been funded over the last decade. These are aimed at the transition to an AOP-based paradigm for chemical safety assessment, with a main focus on the integration of existing *in vivo* data with *in vitro* and *in silico* approaches.[10–13] It has been thoroughly recognised that physiological fluid flow through the liver tissue is one essential prerequisite on the biological side of the coin. Miniaturisation for high throughput at a minimal liver tissue requirement is the other prerequisite on the economical side of the coin. Micro-electro mechanical systems (MEMS) – here called chip-based systems – have been claimed to potentially meet with both of these requirements. Recent general reviews of ''organ-on-a-chip'' and ''body-on-a-chip'' devices describe the technological improvements in this emerging field over the last decade.[14–17] Furthermore, various traditional and novel *in vitro* liver models for toxicity testing, with a particular focus on cell sources involved in liver modelling, were reviewed by Soldatow and colleagues.[18] Finally, an in-depth description of the potential that microfluidic technologies can add to systematic drug toxicity studies was written by Sung and Shuler.[19] In this review, we stress the

[a]*Technische Universität Berlin, Institute of Biotechnology, Department Medical Biotechnology, Gustav-Meyer-Allee 25, 13355 Berlin, Germany. E-mail: eva-maria.materne@tu-berlin.de; Fax: +49 30-314-27914; Tel: +49 30-314-27907*
[b]*Russian Academy of Medical Sciences, Institute of General Pathology and Pathophysiology, Baltiyskaya 8, 125315 Moscow, Russia*

tight relationship between liver architecture and its biological function and, consequently, DILI. We critically review existing chip-based liver equivalents regarding their equivalence to the human liver lobule, the smallest functional unit of the liver. At the end, we sketch a forecast for translational innovations in the field.

Liver architecture and its drug-induced injury

The unique importance of the liver for organismal homeostasis (*e.g.* plasma protein synthesis, glucose biotransformation) and blood detoxification (*e.g.* urea, xenobiotic drug metabolism) has led to a superior evolutionary optimisation of the human liver architecture at the scale of its smallest functional unit – the liver lobule. A precise zonal division of labour along a stretch (500 μm long) of about 25 hepatocytes arranged in cords allow the management of blood detoxification at a blood contact time of only a few seconds. Unsurprisingly, such a superoptimised microfacility is especially vulnerable to inconsistencies, such as toxic effects. This inherent linkage between lobular architecture and the mechanism of DILI requires special attention with regard to the formidable task of providing miniaturised liver equivalents which respond naturally to any toxic agents. Here, we briefly introduce human liver architecture and DILI with a special focus on those elements we believe to be crucial for chip-based equivalents.

Human liver architecture

The liver is the primary site of biotransformation, degradation and detoxification of exogenous and endogenous substances primarily ingested through the gastrointestinal tract. It is built of 1 to 1.5 million hepatic lobules (classic definition), each of cylindrical shape approximately 1.1 mm diameter and 1.7 mm long.[20] Blood from the portal tract, containing the ingested substances, approaches all surfaces of the lobules through a tiny network of capillaries, which restructure into so-called sinusoids (diameter 6–10 μm)[21–24] for plasma contact with hepatocytes in the inner part of the lobules (Fig. 1). After detoxification, blood is collected through a venule in the centre of the cylinder. Portal blood at the entrance mixes with arterial oxygen-rich blood at a ratio of 3 : 1, respectively, to provide oxygen to the liver lobules.[25] The oxygen consumption

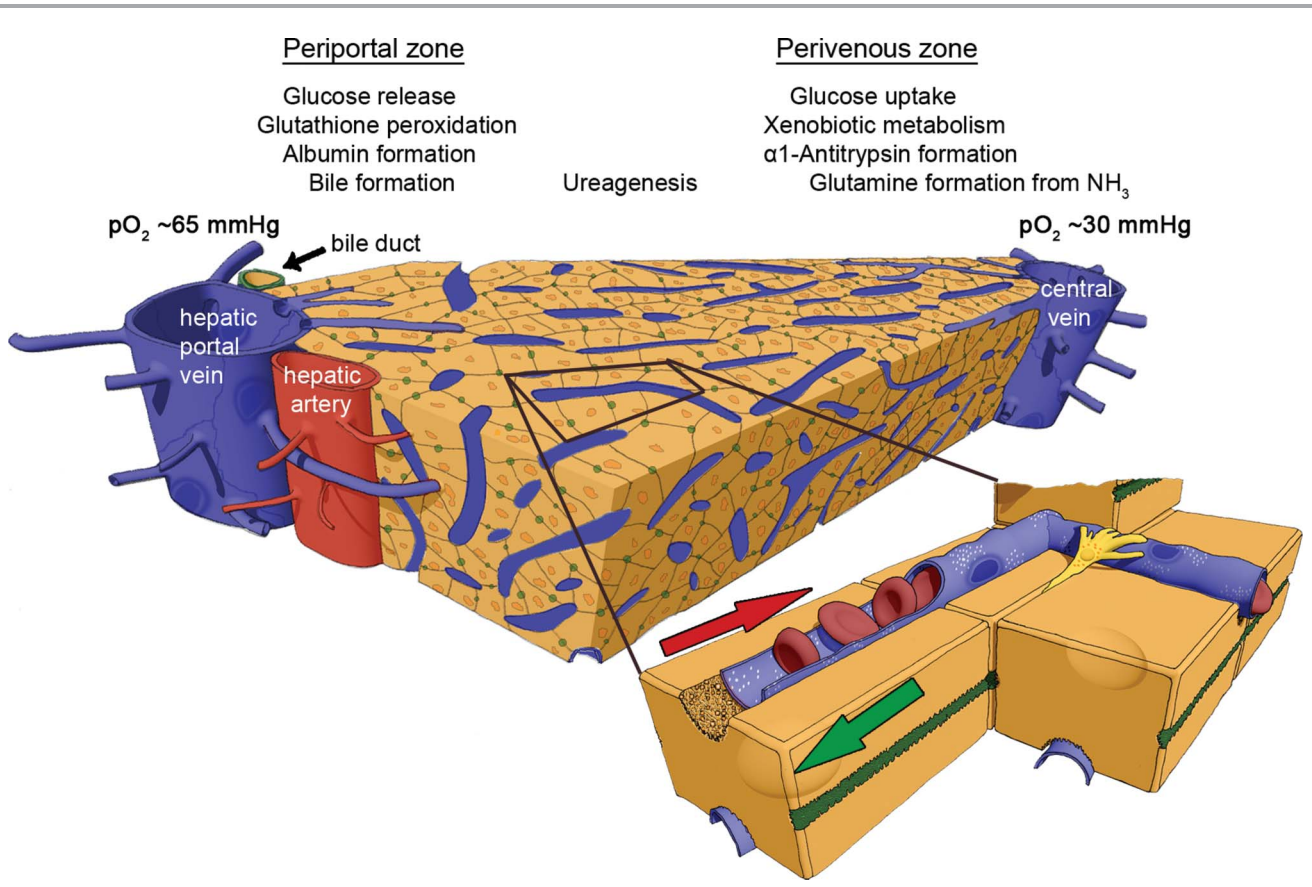

Fig. 1 Liver zonation at lobule level – architecture defines functionality. Periportal and perivenous zonal specialisation of hepatocyte activity is enabled by a sophisticated architecture of the liver lobule – the smallest functional unit of the liver. A stable oxygen gradient is ensured by a dynamic arrangement of blood flow from the outer surface to the centre of the lobule (red arrow), whilst a reverse bile flow takes place in segregated bile canaliculi (green arrow and channels). The space of Disse, generated by tight interactions between liver cells (brownish) and endothelial sinusoids (blue), accounts for efficient substance uptake. Ito cells (yellow) are responsible for matrix formation and remodelling in the space of Disse.

along the approximately 500 μm stretch of blood contact with liver cell cords creates a functionally important oxygen gradient (ΔpO_2 30–35 mmHg).[21] It is evident that the oxygen gradient is a main driver of liver zonation.[26–28] Liver zonation is an evolutionary optimised segregation of the broad liver functions into spatial, temporarily defined, highly specialized zones. This enables hepatocytes of their respective zone to fully concentrate their cellular and molecular capacities onto the single function to which they are dedicated. The distribution of key biotransformation pathways along the cords are highlighted in Fig. 1. This, for example, allows such important processes as albumin synthesis and glucose release in the periportal zone to run separately from, for example, glutamine formation and xenobiotic metabolism in the perivenous zone.[29] As a result of this zonation, DILI events also show a considerable degree of zonal preference depending on the properties of the respective toxic or allergic agent. A detailed listing of substances causing zonal-specific hepatic injury appears in Gebhardt.[27] The centrilobular zone is targeted by acetaminophen,[30] for example.

A single liver lobule contains approximately 10^5 cells in total with a yield and volume distribution as shown in Table 1. The polar hepatocytes are of polygonal shape with approximately 22 μm side lengths arranged in cords. About 37% of the external membrane of the hepatocytes is sinusoidal surface.[20] The absorptive and secretory function of the liver cell is increased six-fold by numerous microvilli, each 0.5 μm in length.[20,31] These microvilli lie in the space of Disse; some even protrude through the fenestrae into the sinusoids and, thereby, have direct contact with the blood.[20,32] The apical surface makes up 15% of the cell's surface area. Neighbouring hepatocytes form bile canaliculi (1–2 μm) by an invagination of their plasma membrane.[31,25] A single hepatocyte has contact with six to ten other hepatocytes. Again, microvilli extend into bile canaliculi to improve bile secretion. The remaining 50% of the hepatocyte membrane is made up of the smooth intercellular fissure, with tight junctions sealing it from the canaliculi and space of Disse.

The prime area of substance uptake is the space of Disse. This is a 0.2 to 1.4 μm wide area[31,21] which connects the hepatocyte cords and the liver sinusoidal endothelial cells, which lack a basement membrane. Plasma approaches the space of Disse through evenly distributed fenestrae. These fenestrae have a diameter of 100 to 200 nm, occur at a frequency of 9–13 per μm^2 and occupy 6–8% of the endothelial surface (see Fig. 1).[33] In addition, soluble macromolecules and colloids of <0.23 μm can be transported from blood through endothelial cells by receptor-mediated endocytosis.[33,34] The hepatic stellate cells (about 5% of liver cells) reside in the space of Disse, are vitamin A-storing pericytes and the main matrix-producing cell type in the liver. Extracellular matrix in the space of Disse is mainly based on fibronectin and collagen. Thick cross-banded collagen type I fibres can be found throughout the whole space. Furthermore, they play an important role in regeneration, associated with angiogenesis and vascular remodelling, differentiation and inflammation.[21,35–38] During liver fibrosis, these cells become activated, acquiring a myofibroblast-like phenotype and starting to produce more extracellular matrix. A thorough review on the origin of these cells, their function in normal liver, and in liver injury and repair can be found elsewhere.[39] Kupffer cells are another important cell type which preferentially reside in the sinusoid of the periportal zone and form almost 80% of the macrophage population. They present antigens and release numerous signalling molecules, which at peak reactivity can lead to hepatic injury. They ingest and degrade aged erythrocytes, bacteria and various endotoxins, and have endocytotic and cytotoxic activity. This population is responsible for allergic DILI. A prime physiological function of Kupffer cells is the induction of tolerance to ingested foreign antigens by immune deviation, active suppression and induction of T cell apoptosis. Their dysfunction may lead to toxic autoimmune responses. Finally, it is important to recognise that hepatocytes in the liver lobule have a natural turnover of 15 days and are capable of rapidly regenerating cord structures after damage.

Summarizing, human liver detoxifies ingested substances within a few seconds along a hepatocyte contact length of 0.5 mm. Plasma contact is mediated by passive filtration and active transport through sinusoidal endothelial cells. This amazing metabolic ability is due to the evolutionarily fine-tuned architecture at liver lobule level. Not much is known about the fluid dynamics of plasma–hepatocyte contact within that interval. The nature of the plasma flow in the space of Disse and the mechanics applied to hepatocytes at these basolateral surfaces are under dispute. The high degree of fenestration may result in the significant transmission of fluid shear stress to hepatocytes. Furthermore, the sinusoids in the periportal zone are of very small diameter at the size of an erythrocyte. Blood cell passage through these tight sinusoids may additionally modulate shear stress. It seems obvious that any specific DILI occurs against the background of the specific local microenvironment, cellular responsiveness and tissue crosstalk in a particular zone of a liver lobule. The emulation of this local spatiotemporal microenvironment or the entire dynamic system seem to be crucial for the ability of any *in vitro* liver model to predict DILI toxicity.

Table 1 Yield and volume distribution of cells within the liver lobule[a]

	Number (% of total)	Volume (% of total)
Hepatocytes	60–65	78
Sinusoidal endothelial cells	10–20	2.8
Kupffer cells	8–12	2.1
Ito (stellate cells)	3–8	1.4
Pit cells	<2	

[a] The extra cellular space accounts for 16% of total liver volume (5% space of Disse, 11% sinusoidal lumina).

Drug induced liver injury – what is the problem?

Two types of DILI have been identified over the last 50 years. Type A, also called intrinsic, is a dose-dependent type of toxicity with a high incidence and short latency. The majority of liver injuries of this type become evident throughout preclinical animal and *in vitro* toxicity studies. Failure to identify at the preclinical stage is responsible for compound

attrition or dose restriction in clinical development. A prime example is acetaminophen, often used as a reference toxicant in *in vitro* studies. Hoehme and colleagues[23] substantiated the crucial importance of hepatocyte–endothelial crosstalk for repair of Type A DILI in mice, establishing an *in silico* model for the repair of drug-induced liver lobule injury. CCl_4 causes hepatocytes close to the central vein to die since only these cells express CYP2E1, which metabolically activates CCl_4 to the toxic entity. This pattern of toxicity is similar to that caused in humans by an overdose of acetaminophen. The model has given unprecedented insights into the dynamics of DILI and regeneration at single liver lobule level in mice. This model has been backed by experimental data and it highlights the exclusive importance of the spatiotemporal interplay of hepatocytes and sinusoidal endothelial cells for proper hepatocyte cord repair after significant perivenous hepatocyte damage in the lobule.

Type B DILI, also called idiosyncratic, is a sporadic dose-independent type of injury which accounts for the majority of hepatotoxicity associated with post-approval medication use. In this stage, it occurs in 1 : 5000 to 1 : 100 000 individuals exposed. It is also evident in the late stages of candidate development, where it causes liver failure, often associated with allergic liver reaction. Each individual case of Type B DILI has significant regulatory impact. A prime example has been AstraZeneca's anticoagulant Exanta (Ximelagatran), which was rejected for approval by the FDA in 2004 and, finally, development was discontinued due to idiosyncratic cases of liver injury.

Numerous efforts have been made in the past to combine the huge volume of widespread knowledge on human liver function, injury and toxicity of chemicals and pharmaceuticals into sound *in silico* models to understand and predict DILI. The most advanced publicly available *in silico* model correlating current state of knowledge into a toolbox for DILI prediction, to our knowledge, is the DILIsym™ human model (http://www.dilisym.com/Products-Services/the-dilisym-model.html) developed at the Hamner-UNC Institute for Drug Safety Sciences, founded under the leadership of Paul Watkins, in North Carolina in 2009. It is designed to be used during drug development to provide an enhanced understanding of the DILI hazard posed by individual molecules and to provide deeper insight into the mechanisms responsible for DILI responses observed at various stages of the development process. A middle-out multi-scale representation of human physiology for assessing potential DILI hazard in patients is provided. It includes key liver cell populations (*e.g.* hepatocytes, Kupffer cells), intracellular biochemical systems (*e.g.* mitochondrial dysfunction) and whole body dynamics (*e.g.* drug distribution and metabolism). Through the generation of SimPops™ (alternate parameterizations of the model with distribution constraints), the DILIsym™ model also includes inter-individual variability. Compound pharmacokinetics (PK) and pharmacodynamics (PD) information can be integrated to predict time profiles of liver enzymes (*i.e.* alanine aminotransferase, aspartate aminotransferase), other clinical variables (*e.g.* bilirubin, prothrombin time) and tissue properties (*e.g.* liver mass, glutathione content). Alternate hypotheses regarding the downstream mechanisms of drug action can be investigated, including increased reactive oxygen/nitrogen species, adenosine triphosphate utilization, direct hepatocyte necrosis, and inhibition of bile acid transporters. Summarising the complex nature of DILI requires *in vitro* prediction models to emulate the full complexity of a liver lobule as closely as possible. This is a formidable challenge for chip-based liver equivalents. Consequently, a stepwise progression of systems, over and above random hepatocyte 3D cultures, towards lobule equivalents is apparent. Table 2

Table 2 Relationship between levels of architectural complexity and biological function of human liver equivalents. Levels B and C are each built upon the preceding level

	Level of architecture	Additional cell types	Additional structure/biology	Corresponding functions	Additional toxicity read-outs
A	Cord-like hepatocyte architecture	None	Hepatocyte polarisation	Artificial basolateral uptake of substances	Responsiveness of polarised hepatocytes
			Formation of bile canaliculi	Separated release of metabolites into apical bile canaliculi	Effect of short-term separation of bile-secreted metabolites from culture medium
			Artificial zonation	Zone specific hepatocyte activity	Activity-related hepatocyte toxicity
B	Endothelial sinusoid architecture	+ Endothelial cells	Formation of apical villi and space of Disse	Physiological basolateral uptake of substance	Hepatotoxicity at physiological uptake levels
			Fenestrated endothelia	Substance filtration/ transport and tissue conditioning	Hepatocyte regeneration along the cords and endothelial cell toxicity
		+ Stellate cells	Disse space stabilization	ECM production	Stellate cell toxicity
C	Entire liver lobule	+ Bile channel epithelia, including oval cells	Bile channels	Complete irreversible segregation of bile from the medium/serum and regeneration potential	Depletion of bile metabolites from the canaliculi system and physiological repair response
		+ Blood	Physiological zonation	Physiological separation of hepatocyte activities into the three zones	Zone-specific intrinsic DILI
		+ Kupffer cells	Sinusoidal dendritic network	Liver-specific immunity	Idiosyncratic DILI

summarises the three architectural levels which would add important specific toxicity read-outs due to higher functionality.

Chip-based liver equivalents for drug testing *in vitro*

A lot of progress has been made in optimising static liver tissue cultures for toxicity testing to a higher level in *in vitro* biology at standard multiwell plate formats compliant with existing liquid handling robotics for high throughput assays. Here, we briefly report on the latest developments aiming to become the next gold standard in industry. In such an assay, liver microtissues of 100–500 μm size are preformed into spheroids or established in matrices and cultured under static conditions. Prime examples are the GravityPlus™ and GravityTRAP™ platforms of InSphero (Zurich, Switzerland) and the RegeneTOX-3D-liver of RegeneMed (San Diego, California, USA). Compliance to robotic liquid handling systems allow for easy daily media exchange and repeated dose substance exposure over weeks. The liver microtissues generated are composed of human primary hepatocytes, co-cultured with non-parenchymal cells, such as endothelial cells or Kupffer cells. It was shown earlier that such microtissues, under optimised static culture conditions, exhibit an artificially optimised microscale architecture that maintains phenotypic functions for several weeks. Their utility for toxicity testing has been demonstrated through the assessment of gene expression profiles, phase I/II metabolism, canalicular transport, secretion of liver-specific products, and susceptibility to hepatotoxins.[40] Such systems do not provide mechanical coupling or physiological morphology, but chemical coupling into oxygen and nutrient gradients has been well demonstrated. Therefore, they serve as the minimum threshold level each microfluidic chip-based liver equivalent should outperform to add value to the toxicity screening landscape. The main features of microfluidic devices – the microscale and physiological fluidics – should translate into more representative liver biology at equal or higher throughput. The well-established fact that non-parenchymal cells are a mandatory part of liver functionality and, therefore, should be applied *in vitro* should be kept in mind.

In the following section, we review the prime microfluidic systems which aim to emulate liver functionality. We screened the literature for chip-based systems and separated them into random hepatocyte 3D cultures and those with higher level architectures. We categorized the latter according to the levels (A–C) introduced in Table 2. We tried to ascertain to which extent they match the corresponding *in vivo*-like functionality. The systems are arranged in the order of their respective level of biological equivalency.

Relevance of cell sources

Standard industrial human *in vitro* liver toxicity studies at high throughput are based on well characterized human cell lines, such as HepG2 and HepaRG.[18,41] Due to their tumorous nature they differ from primary human hepatocytes in various aspects. Therefore, primary human hepatocytes are thought of as the gold-standard for *in vitro* drug metabolism, enzyme induction and toxicity studies.[18] An impressive indicator for their functional superiority is their performance in bioartificial liver assist systems (BALS) successfully bridging the gap for intoxicated liver-failure patients until a transplantation.[42,43] Use of primary hepatocytes combined with a change of cell culture format to 3D and, more importantly, co-cultivation with non-parenchymal liver cells, such as endothelial cells, hepatic stellate cells or Kupffer cells, might improve their cellular and metabolic functions towards *in vivo*-like levels.[22,18,44,45] Induced stem cell technologies, recently awarded with the Nobel Prize in Medicine,[46–49] might provide new solutions to the well described but restricted access to human liver tissue.[50,51]

Random dynamic monocultures

A number of microfluidic liver culture devices exposing hepatocytes in random 3D culture at a lower organisational level have been engineered and will be discussed in this section.

A co-culture system of carcinoma cell line HepG2 with Caco-2 and MCF-7 cells was presented by Imura and colleagues (Fig. 2a).[52,53] The system aims to emulate the hepatic metabolism combined with intestinal absorption for the assessment of human breast carcinoma cell responsiveness to four commonly used drugs. It provides a unidirectional flow in a chip format, the area of a microscope slide, supporting the constant perfusion of 2 to 9 $\times$ 10^5 HepG2 cells cultured on microspheres, corresponding to a cell count of two to nine human liver lobules. Human MCF-7 cell line-based human breast carcinoma cells were consecutively arranged in a single microchannel. Drugs are provided through a fluid-tight monolayer of human Caco-2 cells (intestinal epithelial tumour) into the culture medium flow of the channel in front of the liver compartment. The Caco-2 cell layer mimics the absorptive properties of the human intestine. Exposure was achieved for two days at a flow rate of 0.4 μl min^{-1}, and led to detectable biological effects on the human breast carcinoma cells.[52] A nutrient gradient might occur in the cylindrical vertical part of the hepatocyte culture in the channel. Oxygen should not be limited due to the PDMS nature of the channel. The hepatocyte arrangement on spheres is artificial.

A system developed for pharmacokinetic and pharmacodynamic modelling by Shuler's group[54] (Fig. 2b) has been improved regarding culture format from monolayer hepatocyte cultures to 3D hydrogel supported cultures.[55] It combines cultures of human hepatoma cells HepG2/C3A with colon cancer cells and myeloblasts in separate cell culture chambers. The system, at its selected scale, provides *in vivo*-like tissue mass ratios inside the culture compartments, a culture medium inflow split that is equivalent to the respective blood flow split in humans, and relevant residence times in the tissue compartments. Furthermore, the microfluidic chip design is claimed to support physiological shear stress and liquid-to-cell ratios comparable to those of the respective organs, and it can be operated over periods of up to four days. In order to ensure proper residence times and volumetric

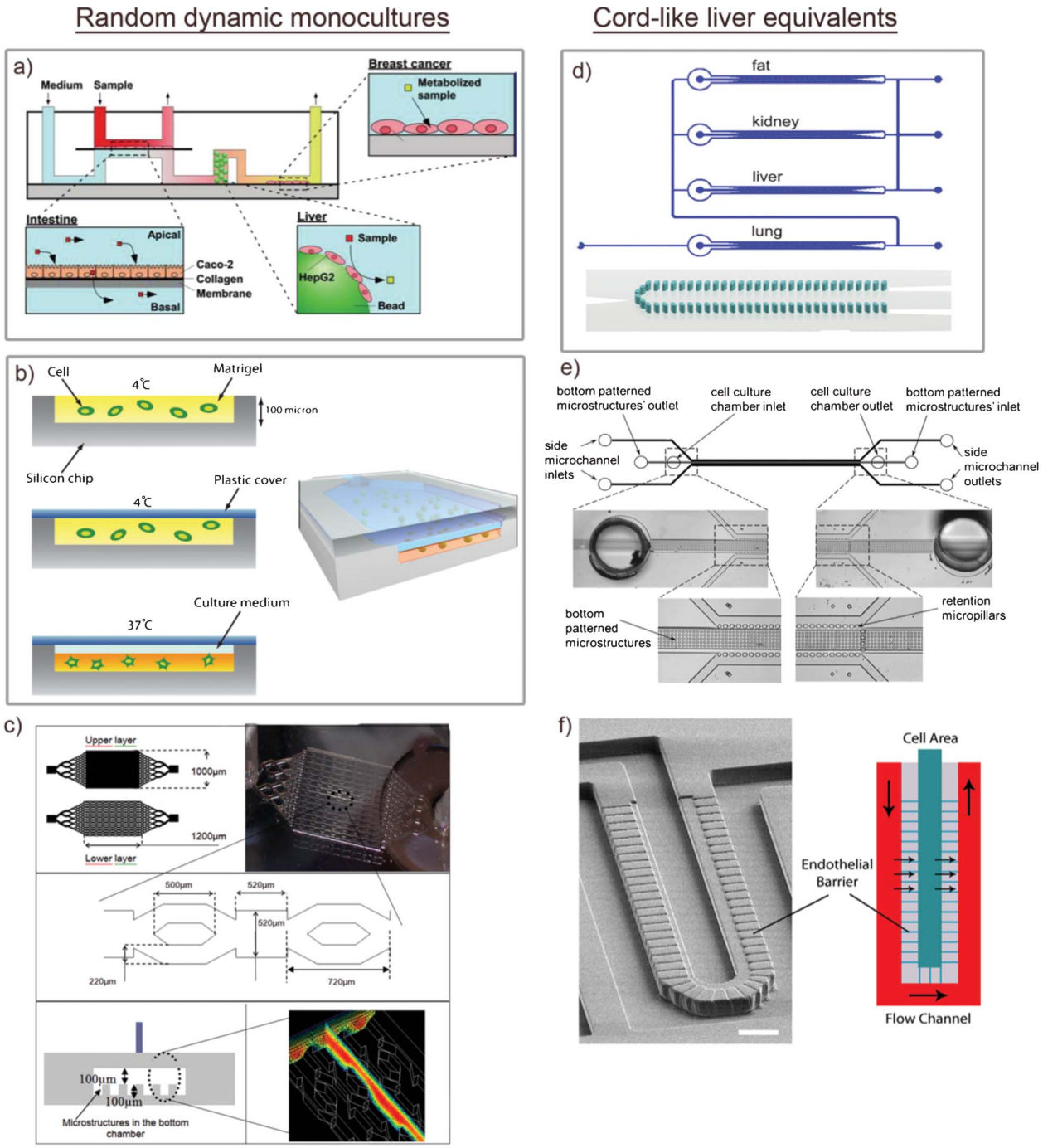

Fig. 2 Metabolically active liver equivalents at elementary architectural level. (a) Schematics of a multi-tissue device exposing hepatocytes on microspheres in a packet cylinder to substances delivered through an intestine barrier. (Reproduced from ref. 52. Copyright 2010 American Chemical Society). A 3D matrigel-based hepatocyte culture, schematically shown in (b), was integrated into μCCA to increase the level of hepatocyte arrangement. (Reproduced from ref. 55 with permission). (c) Schematic layout and perspective view photograph of a chip-based liver equivalent composed of consecutively arranged microchannel geometries with a total surface of 2 cm^2 supporting hepatocyte attachment (0.1–0.5 × 10^6 cell seeding). (Reproduced from ref. 57 with permission of Elsevier). (d) Schematic of a system arranging hepatocytes in a 1 cm cord fluidicly interconnected with other relevant tissues. Shear stress shielding is provided by micropillars as illustrated. (Reproduced from ref. 63 with permission). (e) The schematic layout of another system arranging hepatocytes in cord-like structures, but with additional microstructures at the channel bottom allowing traverse fluid flow. (Reproduced from ref. 66 with permission). (f) Perspective view photograph and schematic of a sieve-pocket-based hepatocyte culture space supporting a cord-like dense package of 250 hepatocytes shielded by a microchannel barrier. (Reproduced from ref. 68. Copyright 2007 John Wiley and Sons). Systems providing a multi-tissue approach are circled in grey.

velocities, the flow rate in that system has been adjusted to a velocity of 168 μm s^{-1} in the liver compartment, which is close to the *in vivo* situation, while cell density and liver compartment architecture are not. The number of liver cells is 10^5, corresponding to one human liver lobule. Apart from the missing architecture, this is one of the few systems which

combines several culture compartments into a combined recirculation supporting molecular crosstalk. To the best of our knowledge, it represents the first and, until recently, the only dynamic microscale system supporting a physiologically based pharmacokinetic, quantitative structure–activity relationship (QSAR) and quantitative *in vitro* to *in vivo* extrapolation modelling.[56]

A system proving acetaminophen sensitivity of 3D clusters of HepG2/C3A cells with four-day activity was developed by Baudoin and colleagues (Fig. 2c).[57] The biochip environment contributed to the upregulation of principal enzymes involved in phase I and II metabolism and phase III transporters.[58] Data suggest superior metabolic activity of the HepG2/C3A cells in comparison to their culture in Petri dishes. A biochip with a culture space of 40 μl contains 1 to 5 × 10^5 hepatocytes, which corresponds to approximately 1 to 5 liver lobules in humans. The system aims for an even and continuous distribution of nutrients and oxygen. Gradients and, consequently, liver tissue zonation was not targeted.

Other systems with lower organizational degrees of hepatocyte cultures not focusing on architectural resemblance are described in the literature, but are not reviewed further here.[59–61]

Cord-like liver equivalents

Since their inception, numerous microfluidic devices have been established for the arrangement and maintenance of hepatocytes in cord-like structures with the potential to ensure physiological hepatocyte polarisation, release of bile into canaliculi and artificial functional zonation. A very interesting system on this level of biology is that of Zhang and colleagues. They developed a microfluidic channel-based system (1 cm long, 200 μm wide, 100 μm high) with an integrated array of micropillars Fig. 2d).[62] About 4 × 10^3 cells per channel were applied, which corresponds to approximately 0.05 liver lobule. Cells were perfusion-seeded into these structures, achieving a high 3D cell–cell interaction. A thin layer of matrix was layered over the 3D cells by a polyelectrolyte complex coacervation process.[63] The cells preserved their 3D cyto-architecture and cell-specific functions for the whole cultivation period of up to one week. The use of intercellular polymeric linkers, such as polyethyleneimine-hydrazide, which stabilise the multicellular aggregates, facilitate the establishment of a more natural extracellular matrix environment.[64] This intercellular linker gradually disappears from the cell surface within two days, allowing the cells to secrete their own matrix. This may promote more *in vivo*-like cellular phenotypes when compared to microfluidic systems incorporating no or exogenous matrices. The integration of gelatin microspheres which released TGF-β1 in a controlled way supported hepatocyte function inside these structures.[65] An increased albumin production and higher phase I and II enzymatic activities, which improved the sensitivity of the hepatocytes to acetaminophen-mediated hepatotoxicity, was shown. In addition to cord-like hepatocyte arrangement, this system allows for the combination of liver cells with other cell types within a common media circulation. It is not obvious if specific zonation characteristics can be stably achieved within the system.[63]

The formation of 3D tissue-like structures composed of polarised cells which form extended bile canalicular structures was presented by Goral and colleagues (Fig. 2e).[66] Cells were seeded in a microfluidic device similar to the one described.[64,62] A series of retention pillars formed a microchannel centred between two side-channels. However, unlike other perfusion-based microdevices, the bottom of the cell culture chamber was patterned with microstructures, which provided an additional control of hepatocyte polarity.[66] In contrast to Toh *et al.*, the channel is 100 μm wide and hosts 10^4 cells, corresponding to 0.1 human liver lobule. Cell culture media could not only be perfused through the cell compartment from the side-channels, but also *via* these patterned microstructures on the bottom, minimising cell spreading and cell–surface interaction. After two weeks of perfusion culture, the cells remained viable and had formed a cord-like structure. An extended bile canalicular structure and the formation of gap junctions between the 3D structured cells could be shown.[66] A clear segregation of bile within the cord structures could be achieved. The patterned microstructures at the bottom are the first step toward technical approaches allowing the separation of bile.

Another cord-like arrangement of hepatocytes could be achieved in a system by Lee and colleagues, additionally aiming to emulate the functions of the space of Disse through a microporous microfluidic barrier (Fig. 2f).[67] Cells were cultured inside a sieved-pocket cell culture area (150 μm wide, 440 μm long) corresponding to 250 densely packed hepatocytes – a very small fraction of a human lobule – without nutrient limitation for over one week. Nutrient depletion was avoided by a continuous maintained flow of medium around the pocket, which diffused across the porous barrier to the cells. It was hypothesized that the flow dynamics of the media may provide necessary cues for hepatocyte differentiation and function.[67] The hepatotoxic effect of diclofenac on human primary hepatocytes cultured in this device could be mimicked.[68] Diclofenac is a model compound for metabolism-mediated hepatotoxicity, as it exhibits its toxic effect only after prolonged exposure (24 h) to metabolically competent cells. Furthermore, the high cell density allowed for an enhanced cell–cell contact with tight junctions and desmosomes. Multi-cellular spheroids were formed that preserved the viability and metabolic activity of the cells over many weeks. This system seems to provide an even distribution of nutrients and oxygen without dynamic oxygen and nutrient gradients important for zonation *in vivo*. Therefore, it might reflect a certain local microenvironment within a lobule. The obvious difficulty in determining cell damage exactly in such small sieve-pockets of 250 cells has been addressed by Meissner and colleagues.[69] They provided a solution for an integrated label-free impedimetric toxicity screening capable of detecting cellular damage in microscale sieve-pockets.

Endothelial sinusoid model and hepatic lobule "equivalent"

The systems mentioned above succeeded in arranging hepatocytes into an artificial but cord-like assembly, restoring hepatocyte polarity and supporting sporadic bile segregation. Co-culture of hepatocytes with non-parenchymal cells in a spatially arranged 3D environment under constant perfusion

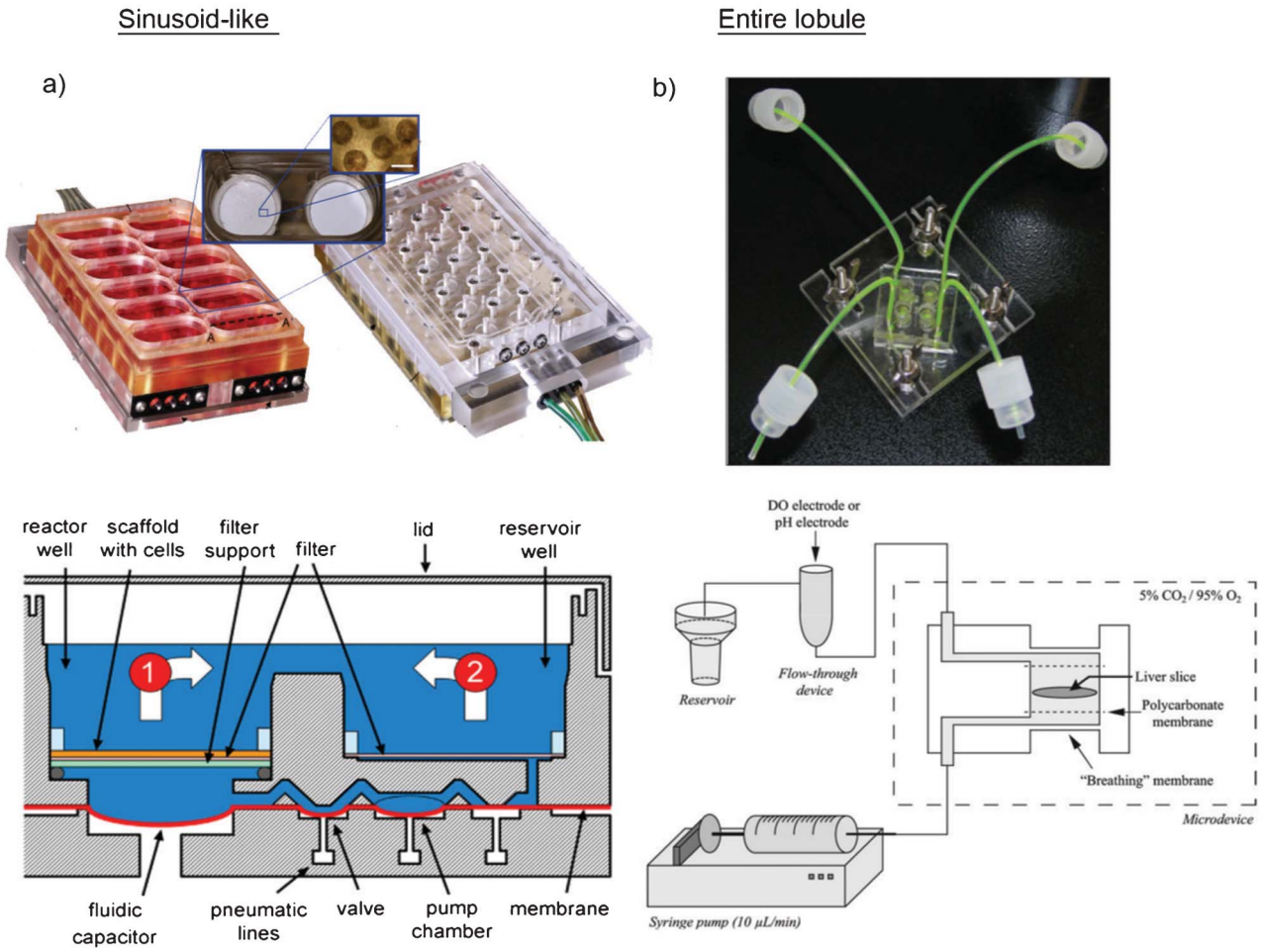

Fig. 3 Systems emulating higher level liver lobule architecture. (a) Perspective view photograph of a parallel multiplate bioreactor hosting 12 liver equivalents and the schematic cross-section of a single liver equivalent culture compartment operated by a peristaltic micropump. A sinusoidal architecture was rebuilt by co-culturing hepatocytes and endothelial cells within microchannels (240 µm long) of a scaffold. Hepatocyte villi and endothelial fenestrae at the hepatocyte endothelial interface, observed in electron micrograph, substantiated sinusoidal architecture. (Reprinted from ref. 70 with permission). (b) Perspective view photograph of a microfluidic biochip hosting 4 liver equivalents and schematic layout of a single perfusion culture for a 100 µm × 4 mm precision cut liver slice initially comprising the physiological architecture of a part of a liver lobule, although heavily damaged. (Reproduced from ref. 71. Copyright 2010 John Wiley and Sons).

might lead to the formation of basolateral villi and space of Disse on the background of fenestrated endothelia – a next level of architectural resemblance to the *in vivo* situation. A very interesting approach to modelling sinusoid like structures in a microfluidic system has been developed by Domansky and colleagues (Fig. 3a).[70] An array of multiple bioreactors was build into a multiwell plate comprising 12 autonomous microfluidic systems, each being perfused by an integrated pneumatic micropump circulating a total volume of 3 ml. Each tissue culture scaffold contains 769 multichannels (0.24 mm deep, 0.34 mm diameter) and was seeded with 10^6 rat hepatocytes and endothelial cells at a 1 : 1 ratio. With regard to hepatocyte numbers, this corresponds to approximately 10 human liver lobules. A continuous adjustable oxygen gradient could be established over long operating times. The scaffold supports near physiological tissue densities and the functional zonation of hepatocytes can be stipulated. The large channels of the scaffold support self-assembly of the two cell types in dynamic conditions. Liver sinusoid endothelial cells, known to lose their differentiated phenotype *in vitro*, maintained the expression of the functional marker SE-1 throughout the culture.[70] The important features of adjustable flow rates on the basis of an oxygen consumption model, long-term steady gradient maintenance and the ability for co-culture of hepatocytes with different types of non-parenchymal cells made the system an interesting alternative for toxicity testing.

The highest level of architecture – the entire liver lobule – has not yet been reached, but a chip-based microfluidic approach to contain a major part of a liver lobule has been made by van Midwoud and colleagues (Fig. 3b), who cultivated 3 mg of liver slice tissue. The precision cut liver slice (100 µm thick, 4 mm diameter) was perfused by a 10 µl min^{-1} media flow in an incubator chamber with constant pH and dissolved oxygen.[71] In a human setting, the tissue used here would correspond to approximately two liver lobules (around 2×10^5 liver cells). Biotransformation activity was shown to be equal in control slices in static culture over three hours. The system does not demonstrate any advantage with regard to metabolic

functionality over the three-hour measurement time. The authors highlight the advantage of continuous media perfusion at low tissue-to-fluid volume ratios in contrast to steady metabolite accumulation in static culture. Unfortunately, data on the culture performance over longer times than 72 h are not presented.[72] Although the lobules' architecture within the tissue was preserved, the artificial media perfusion is not able to eventually provide a dynamic oxygen gradient and, consequently, spatiotemporal zonation. Finally, the system does not assist the segregation of bile and media flow. The only other example in the literature of maintaining liver tissue slices in a microfluidic arrangement has been published by Hattersley and colleagues.[73] The authors succeeded in maintaining viable liver slices 71 h with albumin secretion varying in a cyclic manner peaking every 24 h and urea remaining relatively stable.

To the best of our knowledge, no other microfluidic devices have been described which apply complex liver lobule tissue biopsies or create this complexity in the systems and, furthermore, show this degree of tissue viability. Neither of these hepatic lobule ''equivalents'' provides a physiological connection of an entire liver lobule to a surrogate of a blood microcirculation and bile removal. Therefore, the achievement of improved functionality and toxicity read-outs highlighted in Table 2 are not possible.

Complex organotypicalness *versus* cost-efficient throughput

We have plotted a representative array of existing chip-based liver equivalents for drug toxicity testing against the level of human biology they try to emulate (Table 2).

None of the systems developed to date ultimately mirrors the architecture of a human liver lobule at full-scale complexity. However significant improvements towards higher levels of functionality and, consequently, toxicity read-outs have been made with cord-like architectures. Chip-based liver tissue slice culture and a sinusoid liver model co-culturing hepatocytes and endothelial cells under fluid flow shear stress are the most advanced systems with regard to the organisational complexity of cultured tissues. The former is at a very early research level with irrelevantly short operational time. The latter has been transferred from research[74–76] into a LiverChip perfusion plate (Zyoxel, Cambridge, UK). This commercial system is well characterised with regard to metabolism and function related to toxicity. It is designed to support toxicity evaluation over at least three weeks. We identified a second commercially available microfluidic liver equivalent system – the Pearl microfluidic perfusion array (CellAsic, Hayward, California, USA). It works with passive unidirectional perfusion (100 μl day^{-1}) with 32 samples (25 000 cells each) on a 96-well plate format over 30 days with hepatocytes being shielded from shear stress by an endothelial sieve surrogate. Human hepatocytes are concentrated into high density cords and provided with oxygen through air diffusion channels. Porous ''sinusoid'' channels run in between cell regions comparable to those reported by Lee and colleagues described above. Finally, HμREL*flow*™, a system based on the μCCA of Shuler and colleagues, described above, seemed to be commercially available (HμRel corporation, Beverly Hills, California USA). To the best of our knowledge, these are the only three microfluidic devices on the market consisting of human liver equivalents for toxicity testing; their robust validation and comparison with static liver microtissue culture systems, such as GravityPlus™ and RegeneTOX-3D-liver described above, have not yet been completed by the pharmaceutical industry. It is worth noting that the level of automated parameter control, such as in-process controls of pH and pO_2, of the chip-based liver equivalents reviewed here do not compare with the advanced macroscale bioartificial liver-assist systems used at the patient's bedside, and the corresponding hollow fibre-based research liver bioreactor system of Zeilinger and colleagues.[77,78]

With regard to the commercial element, throughput and costs, the features listed in Table 3 highlight two obvious facts: (i) The liver equivalent number operated by the devices reported is far from being compliant with high throughput requirements, and (ii) ensuring circulating fluid flow in liver equivalents requires pump systems with control units attached. Any such addition of technical equipment to operate the chip-based liver equivalents, limits their throughput capacity at increasing costs per single test point.

Nowadays, drug candidates undergo a finely tuned multi-step characterisation and selection process from discovery to market approval. A rapidly decreasing gradient of test throughput applies to that process to select a single successful candidate out of about 10 000 initial compounds. Simultaneously, costs associated with the development of a single entity to market approval, rapidly increase at late stage development associated with clinical trial expenditures. The

Table 3 Key parameters of reviewed chip-based liver equivalents

Biological complexity	Cultures per device	Cells per culture	Density (cells cm^{-3})[a]	Chip volume	Co-culture	Multi-tissue	Circulating medium	Reference
Hepatic lobule equivalent	4	2×10^5	3×10^8	0.6 ml h^{-1}	Yes	No	No	71
Endothelial sinusoid model	12	10^6	0.5×10^8	15 ml h^{-1}	Yes	No	Yes	70
Cord-like liver equivalents	1	250	2×10^8	0.6–1.2 μl h^{-1}	No	No	No	68
Cord-like liver equivalents	1	10^4	10^9	5 μl h^{-1}	No	No	No	66
Cord-like liver equivalents	1	$\sim 4 \times 10^3$	1.8×10^7	200 μl h^{-1}	No	Yes	No	63
Random dynamic monocultures	1	$0.1–0.5 \times 10^6$	3×10^7	up to 1.5 ml h^{-1}	No	No	Yes	57
Random dynamic monocultures	6	10^5	10^7	160 μm s^{-1}	No	Yes	Yes	55
Random dynamic monocultures	1	$2–9 \times 10^5$	3.75×10^7	24 μl h^{-1}	No	Yes	No	52

[a] *In vivo* cell densities in liver lobules corresponds to 3×10^8 cells cm^{-3}.

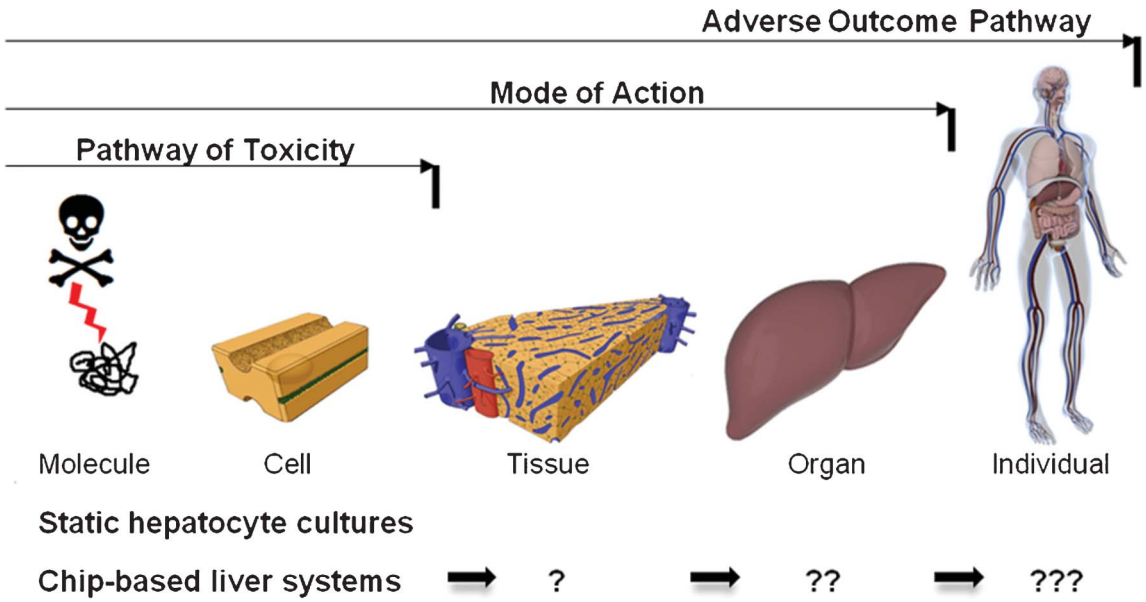

Fig. 4 The adverse outcome pathway paradigm in safety assessment. According to the AOP paradigm, the value of *in vitro* methods to predict DILI increases with the degree of emulation of the liver (MoA level) or the human body as a whole (AOP level). Chip-based liver equivalents, reviewed here, have made the first early progress into liver lobule modelling. With the translational improvement of MEMS technologies, full-scale emulation of human liver lobules and, finally, ''Human-on-a-chip'' devices may raise preclinical prediction of DILI to a historical score.

major high throughput burden is at the stage of early discovery, it goes down to several hundred test animals per compound in the preclinical toxicity stage and rarely more than 50–60 human test volunteers in the clinical safety assessment stage (Phase 1). Clinical efficacy evaluation (Phases 2 and 3) usually requires several thousand patients. Intrinsic DILIs cause attrition rates in early clinical development, whilst idiosyncratic DILI appears in late clinical trials as the cohorts increase in size. There is no further economical playground to increase preclinical costs unless a significant move toward human biology and predictiveness is made. All systems reviewed here are at an early stage and require validation prior to use in routine toxicity screening. Advanced high throughput compliant static 3D liver cultures are the benchmark chip-based human liver models have to outperform at equal or lower price if the added value is incremental. Only translational solutions to the toxicity dilemma legitimise higher level expenditures.

Many hurdles

Screening the current picture, we have identified that chip-based liver equivalents for toxicity testing are at a very early research stage of their development. A broad variety of system designs operated with very different process parameters exist. Therefore, microfluidic platforms aiming to add value to liver toxicity testing of pharmaceutical entities still face major challenges. Here, we discuss possible approaches to step into the future.

Status quo and fit with modern toxicity requirements

Nowadays, the pharmaceutical and consumer industries face a paradigm shift in their safety assessment strategies. The dire need to quickly and efficiently select potential hits for toxicity is a potent driver for the implementation of *in vitro* assays emulating a higher degree of human biology. This is backed by the US FDA, quoting FDA commissioner Margaret A. Hamburg: ''We must bring 21st century approaches to 21st century products and problems. Toxicology is a prime example. We need better predictive models to identify concerns earlier in the product development process to reduce time and costs.''[79] It implies a transition to an AOP-based paradigm for safety assessment in toxicology. This paradigm, schematically outlined in Fig. 4, implies that an initiating molecular event, caused by a toxic agent leads to a series of consequences on at least three levels of biological complexity to finally end up with the undesired adverse outcome.

The agent-specific adverse outcome pathway includes all three levels:

i. The molecular interaction with a receptor, DNA or protein inducing, *e.g.* gene activation, altered signalling or protein production or depletion at a cellular level, representing the pathway of toxicity (PoT) of the toxic agent;

ii. alteration of physiological function, disrupted local homeostasis and altered local tissue development, *e.g.* liver fibrosis at tissue and organ level, i and ii together representing the mode of action (MoA) of the toxic agent;

iii. and finally, multi-organ failure and lethality or impaired development and reproduction, i, ii and iii together representing the adverse outcome pathway (AOP) of the respective toxic agent.

Conventional static liver cultures and random dynamic chip-based hepatocyte cultures, nowadays, support the identification of pathways of toxicity restricted to acute toxicity due to limited substance exposure times and lack of architectural complexity *in vitro*. With the growing complexity of liver equivalents *in vitro* and rising robustness of tissue maintenance over long periods, MoA analysis may come within reach both for acute and chronic toxicity at repeated doses. The endothelial sinusoid and liver lobule emulating microfluidic devices reviewed here are the very first step in this direction. Chip-based entire liver lobule equivalents bear the potential to fully emulate DILI at the single organ level *in vitro* in the future. Finally, none of the three architectural levels for chip-based liver equivalents, summarised in Table 2, would be able to emulate the AOP of DILI in other organs within an entire organism.

Prospective improvements of existing chip-based liver equivalents

We have outlined three architectural levels for human chip-based liver equivalents which each consequently add a critical functional feature of human liver and might significantly improve the predictiveness of toxicity testing in comparison to random static and dynamic 3D hepatocyte culture. The following improvements of existing systems might optimise their performance.

Level A – cord-like hepatocyte architecture: chip-based systems of this category should be optimised towards the accurate establishment of an artificial zonation along the cords. Therefore, the measurement of the local oxygen gradient and monitoring of single hepatocyte viability, for example, by live tissue imaging techniques, would be advantageous. Investigation into the ratio of basolateral (absorption) *versus* apical (bile release) surfaces within the cords might allow comparison with the *in vivo* situation in man.

Level B – endothelial sinusoid architecture: in addition to the optimisation suggested for level A liver equivalents, we propose the integration of stellate cells at physiological ratios into endothelial sinusoids *in vitro*. Investigation into spatially coordinated proliferation of hepatocytes along the sinusoids in response to toxic cell losses would prove the added value of such chip-based liver equivalents for repeated dose toxicity evaluation. Moreover, it would be interesting to use such systems in order to discover the biological cues inducing villi formation on hepatocytes and fenester formation on endothelial cells in human liver.

Level C – entire liver lobule: adding to the aforementioned improvements of level A and B, physiological lobule-like zonation of primary hepatocyte cords induced by blood perfusion and segregation of bile from canaliculi into separate channels would be the next breakthrough at this level of human liver equivalents. The first aims for natural zonal hepatocyte specialisation allowing differentiating individual PoTs of a toxic agent, *e.g.* reactive metabolite toxicity and mitochondrial impairment at physiological levels of hepatocyte activity. The second would foster the identification of toxic agents, inducing intrahepatic choleostasis modulating bile transport systems. The inclusion of an immune system – Kupffer cells – would be another important improvement which would aim for the detection of allergic idiosyncratic DILIs. Finally, the construction of biological bile channel covered by epithelial cells, including oval cells, would add important liver repair functionality crucial to predictive toxicity testing.

Furthermore, the extension of the multi-tissue systems reported here at level A in the direction of systems physiologically arranging an intestine and a kidney equivalent with a liver equivalent on a chip may enable a new application for multi-tissue liver equivalents – the generation of ADME data and PK/PD analysis within one experimental setting.

We recommend the generation of a biological baseline for any chip-based liver equivalent, leading, in a first step, to the eventual transfer of a chip-based liver equivalent into industrial use. It is necessary, therefore, to determine the architectural and functional correlation of the chip-based liver equivalent with the *in vivo* liver based on histology, analysis of gene expression, protein levels, such as albumin secretion, CYP450 (selected protein activities – CYP1A, CYP2C, CYP3A), ATP, GSH, LDH, AST, ALT, and metabolite analysis. We further recommend the generation of an extensive time course of both early and late time points and to compare it with data of standard or advanced static hepatocyte cultures.

In a second step, hepatotoxicants should be assessed by the chip-based liver equivalents to prove that additional MoA data beyond PoTs can be derived at the different levels in contrast to the static and dynamic random hepatocyte models. We would advise the use of early and late time points and, if possible, pharmacologically relevant doses. The same read-outs as those set out in step one could be applied. Toxic agents might, for example, include acetaminophen, tetracycline statins or ketoprofen. The application of reversed dosimetrics with QSAR-estimated partitioning coefficients and metabolism parameters[80,81] will allow human-relevant data to be derived from these assessments.

In addition to the improvements in the three levels of biology on a chip, actuators and sensors operating and controlling the chip-based liver equivalents should be improved for repeated dose long-term toxicity testing. In-process monitoring and control for the pO_2 gradient along the cords and pH is mandatory for robust toxicity evaluation. It is an important part of any of these developments to interact with available information tools such as the DILIsym *in silico* platform, extracting existing knowledge and feeding its own data.

We believe that industrially validated test assay platforms for short-term exposure safety assessment might evolve from any of the ongoing chip-based liver equivalent developments at any of the three levels. This will identify toxic agents earlier in discovery, shortening development timelines and eventually reducing acute systemic toxicity testing in animals. Optimisation toward standardised cost-effective automated handling should be a prime focus in order to meet high industrial throughput requirements at competitive costs.

"Humans-on-a-chip" to evaluate AOPs – the ultimate level?

Even an entire chip-based liver lobule equivalent (Table 2 level C) differs from human biology in a pivotal aspect: The inability

to emulate the AOP of DILI in other organs within an entire organism. Therefore, it will be necessary to climb to the next level of systemic biology – long-term homeostasis of primary organoids at a miniaturised organismal level *in vitro*. Given an ethically acceptable supply of the necessary human tissues, by carefully weighing ethical issues against medical needs, ''human-on-a-chip'' systems that provide unlimited homeostasis and organoid repair capability on the basis of biological vascularisation, physiological blood perfusion and the maintenance of organ-specific stem cell niches, could be a translational approach, which we have laid out elsewhere.[17] In brief, human endothelial cell-based blood vasculature should, therefore, form and interconnect several microvascular beds into a common blood circulation. Each of the microvascular beds needs to be integrated into an organ-specific stromal tissue bed, which provides the respective extracellular matrix-based microarchitecture for proper organoid assembly. Orchestrated organ-specific groups of fully functional organoids should maintain their specific functions in concert. The concept is based on the fact that almost all human organs are assembled from multiple, identical and functionally self-reliant structural units, *e.g.* the liver lobule, which perform the most prominent functions of the particular organ. The multiplication of these structures, which have been named organoids, within a given organ is nature's risk management tool to prevent a total loss of functionality during partial organ damage. With regard to evolution, this concept has allowed organ size and shape to be easily adjusted to the needs of a given species – for example, the liver in mice and men – while following nearly the same arrangement to build up single functional organoids. It is important that these organoids are of very small dimensions, from several cell layers up to a few millimetres. The reactivity of organoids to drugs and biologics is supposed to be representative of the whole organ because of their distinguished functionality and a high degree of self-reliance within the respective organ. Therefore, a prime approach to fully emulate human organs at a minimum scale of at least a single organoid per organ (less than 2 μl) might be the development of vascularised blood-perfused chips supporting an organoid on-chip assembly within the right microenvironment. Fig. 5 shows an example of this ''human-on-a-chip'' concept developed to fit the multi-organ-chip format the area of a standard microscope slide, developed in our labs.[17] At this chip scale, we are aiming to operate a ''human-on-a-chip'' 100 000-fold smaller than its *in vivo* counterpart. Therefore, the liver equivalent is designed to host ten human liver lobules. All the other organ compartments are designed to hold a number of their organoids that is proportional to the ten liver lobules.

The biological level proposed here is a desperate challenge. It demands, among other things, the provision of actuators and sensors for the ''human-on-a-chip'' platforms that match the functions of their *in vivo* counterparts. Actuators should couple a broad range of mechanical stresses differentially into relevant organs, at natural degrees. Sensors with exceptionally high sensitivity should be developed to detect the main parameters of human organismal homeostasis, such as: organ viability, tissue temperature, pH, daily fluid balance, intracapillary pressure, blood flow volume, oxygen and nutrient consumption, fluid adsorption and intestinal juice secretion, albumin and bile synthesis, urea excretion, ion balances, osmolarity, and electrical coupling in the minute sample volumes derived from such a miniaturised microfluidic device. Miniature organ sizes and contact-free access to the transparent bottom of the chips might allow the use of strong in-process research tools, such as, two-photon microscopy for tissue imaging, fluorescence ratio imaging for local interstitial pH measurement,[82] phosphorescence quenching microscopy for interstitial pO_2, or infrared spectroscopy to detect physiological stresses.[83] Systems biology approaches for the identification of physiological performance, or adverse outcome pathways at stress overloads, might be applied on samples daily.[84] A few years ago, such a target seemed to be pure science fiction, but the unprecedented joint development programme between the NIH, DARPA and the FDA (http://www.ncats.nih.gov/research/reengineering/tissue-chip/tissue-chip.html), initiated in 2012, to develop ''human-on-a-chip'' systems combining ten human systems/organs on a single chip is a unique hallmark, indicating the translational impact of such concepts on the drug development pipeline. The programme has identified leading research groups that are focusing on chip-based disease model development within the USA. This is an attractive opportunity to create new research alliances among all the partners within the field to convert this vision into a reality. Such a significant move towards individualised ''humans-on-a-chip'' justifies substantial development and test costs, as it may be rewarded by the ultimate decrease of attrition rates in clinical trials. The forecasted complexity of such systems at large throughput might potentially offer a platform to even identify idiosyncratic DILI prior to human trials. Finally, it remains wishful thinking to expect such a ''homunculus'' (small man) on-a-chip to develop, for example, consciousness. One must always keep in mind that the term ''human'' in ''human-on-a-chip'' has the meaning of an artificial copy, effigy or image. The uniqueness of a human being is inviolable.

Concluding remarks

The development of chip-based liver equivalents for toxicity testing is at a very early research stage of development. None of the currently existing systems reviewed here fully matches the architectural complexity of a human liver lobule, with precision cut tissue slices being the closest. Only a few chip-based equivalents, to a certain degree, emulate lower level complexities, such as hepatocyte cords and sinusoidal architecture. It is important to note that at least two microfluidic liver equivalents have already made it into commercialisation. Their advantages in comparison to advanced static 3D liver test systems have yet to be demonstrated by the ongoing feasibility studies in pharmaceutical companies. The existing microfluidic liver equivalent platforms represent a perfect basis for further improvement into chip-based liver equivalents providing stable controllable zonation of hepatocyte cords and segregation of bile. Furthermore, the combination of the liver equivalents with

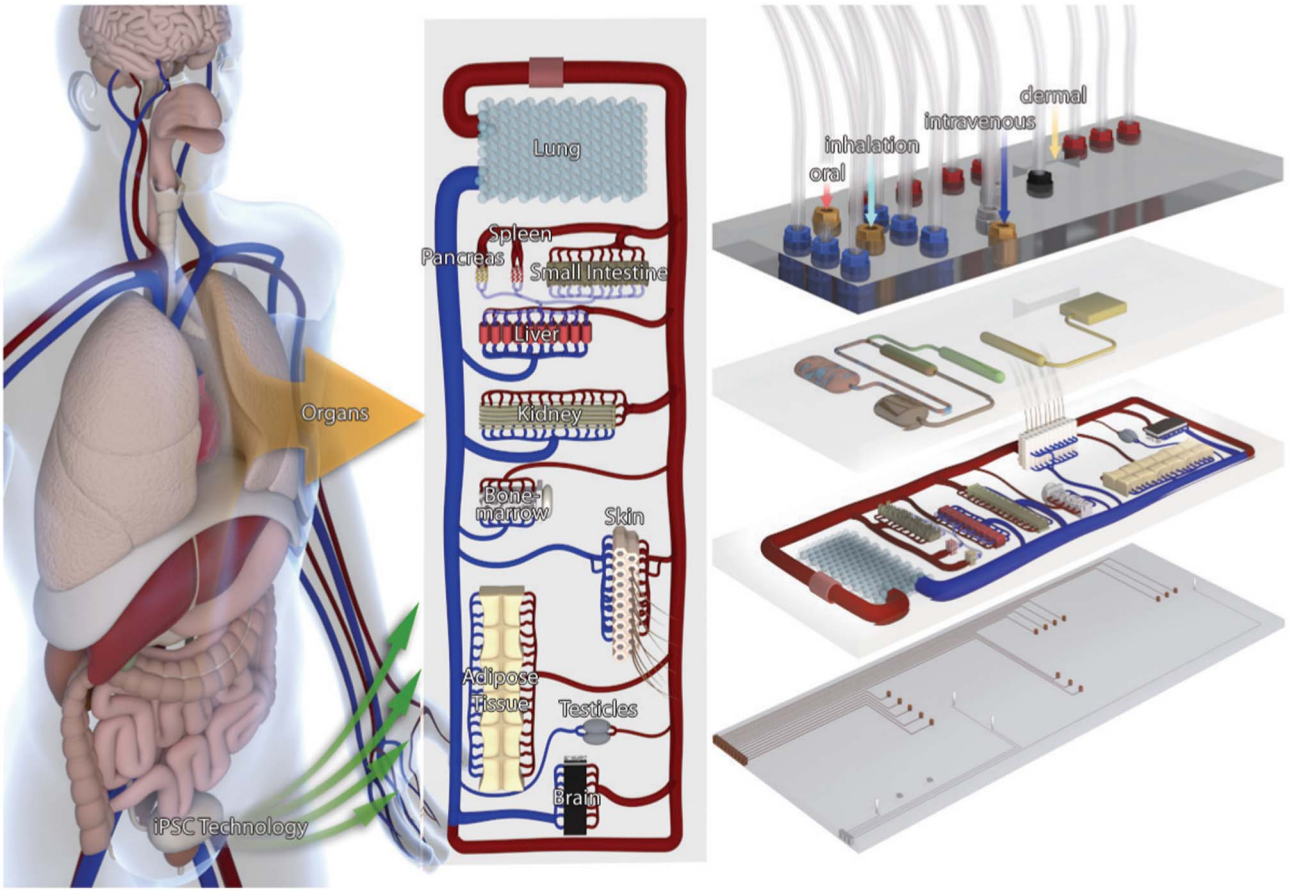

Fig. 5 ''Man-on-a-chip'' at 0.00001 scale. Here is a possible design for maintaining 11 human organ equivalents (middle top view) in a common blood vasculature on a chip the area of a standard microscope slide. The microfluidic device (right side) consists of sensors, organ equivalents, antra for nutrition, bile excretion, urine and faeces removal, and actuators providing mechanical cues for heartbeat, peristaltic intestinal movement, lung air-flow, bone compression, arteriolar constriction, and urine and bile removal. Access points for substance exposure through the different routes are highlighted. Finally, the use of pluripotent stem cell technologies for the supply of different tissues of one and the same donor instead of biopsies from each organ is accentuated in the left. This technology allows differentiating respective tissues from induced stem cells generated for example from adipose tissues.

intestine and kidney equivalents may result in chip-based systems for ADME-Tox testing. Finally, to fully elaborate on the unique features of MEMS technologies, a forecast towards ''Humans-on-a-chip'' to predict AOPs for DILI at the level of the individual organism has been sketched.

Acknowledgements

We thank Andreas Schwarz and Peter Mangel for the creative help with Fig. 1 and 5, respectively. Finally, the review would not exist with the outstanding creative assistance of Philip Saunders and Silke Hoffmann.

References

1 United Nations, *Consolidated List of Products Whose Consumption and/or Sale Have Been Banned, Withdrawn, Severely Restricted or not Approved by Governments Fourteenth Issue*, 2009, 14th edition.
2 United Nations, *Consolidated List of Products-Whose Consumption and/or sale have been banned, withdrawn, severely restricted or not approved by Governments*, 2005, 12th edition.
3 S. M. Paul, D. S. Mytelka, C. T. Dunwiddie, C. C. Persinger, B. H. Munos, S. R. Lindborg and A. L. Schacht, *Nat. Rev. Drug Discov.*, 2010, **9**, 203–14.
4 Food Drug Administration, *Guidance for Industry Drug-Induced Liver Injury: Premarketing Clinical Evaluation*, 2009.
5 G. T. Ankley, R. S. Bennett, R. J. Erickson, D. J. Hoff, M. W. Hornung, R. D. Johnson, D. R. Mount, J. W. Nichols, C. L. Russom, P. K. Schmieder, J. A. Serrrano, J. E. Tietge and D. L. Villeneuve, *Environ. Toxicol. Chem.*, 2010, **29**, 730–41.
6 S. Gibb, *Reprod. Toxicol.*, 2008, **25**, 136–8.
7 F. S. Collins, G. M. Gray and J. R. Bucher, *Science*, 2008, **319**, 906–907.
8 D. Krewski, M. Westphal, M. Al-Zoughool, M. C. Croteau and M. E. Andersen, *Annu. Rev. Public Health*, 2011, **32**, 161–78.
9 D. J. Dix, K. A. Houck, M. T. Martin, A. M. Richard, R. W. Setzer and R. J. Kavlock, *Toxicol. Sci.*, 2007, **95**, 5–12.

10 D. Basketter, J. Crozier, B. Hubesch, I. Manou, A. Mehling and J. Scheel, *Regul. Toxicol. Pharmacol.*, 2012, **64**, 9–16.
11 T. Hartung, B. J. Blaauboer, S. Bosgra, E. Carney, J. Coenen, R. B. Conolly, E. Corsini, S. Green, E. M. Faustman, A. Gaspari, M. Hayashi, A. Wallace Hayes, J. G. Hengstler, L. E. Knudsen, T. B. Knudsen, J. M. McKim, W. Pfaller and E. L. Roggen, *Altex*, 2011, **28**, 183–209.
12 S. Adler, D. Basketter, S. Creton, O. Pelkonen, J. van Benthem, V. Zuang, K. E. Andersen, A. Angers-Loustau, A. Aptula, A. Bal-Price, E. Benfenati, U. Bernauer, J. Bessems, F. Y. Bois, A. Boobis, E. Brandon, S. Bremer, T. Broschard, S. Casati, S. Coecke, R. Corvi, M. Cronin, G. Daston, W. Dekant, S. Felter, E. Grignard, U. Gundert-Remy, T. Heinonen, I. Kimber, J. Kleinjans, H. Komulainen, R. Kreiling, J. Kreysa, S. B. Leite, G. Loizou, G. Maxwell, P. Mazzatorta, S. Munn, S. Pfuhler, P. Phrakonkham, A. Piersma, A. Poth, P. Prieto, G. Repetto, V. Rogiers, G. Schoeters, M. Schwarz, R. Serafimova, H. Tähti, E. Testai, J. van Delft, H. van Loveren, M. Vinken, A. Worth and J.-M. Zaldivar, *Arch. Toxicol.*, 2011, **85**, 367–485.
13 I. Kimber, C. Humphris, C. Westmoreland, N. Alepee, G. D. Negro and I. Manou, *J. Appl. Toxicol.*, 2011, **31**, 206–9.
14 M. B. Esch, T. L. King and M. L. Shuler, *Annu. Rev. Biomed. Eng.*, 2011, **13**, 55–72.
15 D. Huh, G. A. Hamilton and D. E. Ingber, *Trends Cell Biol.*, 2011, **21**, 745–54.
16 C. Moraes, G. Mehta, S. C. Lesher-Perez and S. Takayama, *Ann. Biomed. Eng.*, 2012, **40**, 1211–27.
17 U. Marx, H. Walles, S. Hoffmann, G. Lindner, R. Horland, F. Sonntag, U. Klotzbach, D. Sakharov, A. Tonevitsky and R. Lauster, *Altern. Lab. Anim.*, 2012, **40**, 235–57.
18 V. Y. Soldatow, E. L. LeCluyse, L. G. Griffith and I. Rusyn, *Toxicol. Res.*, 2013, **2**, 23.
19 J. H. Sung and M. L. Shuler, *Bioprocess Biosyst. Eng.*, 2010, **33**, 5–19.
20 H.-D. K. E. Kuntz, *Hepatology: Textbook and Atlas*, Springer Medizin Verlag, Heidelberg, 2008.
21 Y. Nahmias, F. Berthiaume and M. L. Yarmush, Integration of technologies for hepatic tissue engineering, in *Advanced Biochemical Engineering*, vol. 103, ed. K. Lee and D. Kaplan, Springer, Berlin Heidelberg, 2006, pp. 309–329.
22 M. L. Yarmush, M. Toner, J. C. Dunn, A. Rotem, A. Hubel and R. G. Tompkins, *Ann. N. Y. Acad. Sci.*, 1992, **665**, 238–52.
23 S. Hoehme, M. Brulport, A. Bauer, E. Bedawy, W. Schormann, M. Hermes, V. Puppe, R. Gebhardt, S. Zellmer, M. Schwarz, E. Bockamp, T. Timmel, J. G. Hengstler and D. Drasdo, *Prediction and validation of cell alignment along microvessels as order principle to restore tissue architecture in liver regeneration*, National Academy of Science, Washington, 2010, vol. 107.
24 G. Puhl, K. D. Schaser, B. Vollmar, M. D. Menger and U. Settmacher, *Transplantation*, 2003, **75**, 756–61.
25 J. Sear, *Baillieres Clin. Anaesthesiol.*, 1992, **6**, 697–727.
26 K. Jungermann and N. Katz, *Hepatology*, 1982, **2**, 385–95.
27 R. Gebhardt, *Pharmacol. Ther.*, 1992, **53**, 275–354.
28 A. J. Davidson, M. J. Ellis and J. B. Chaudhuri, *Biotechnol. Bioeng.*, 2012, **109**, 234–43.
29 K. Jungermann and T. Kietzmann, *Annu. Rev.*, 1996, 179–203.
30 J. G. Bessems and N. P. Vermeulen, *Crit. Rev. Toxicol.*, 2001, **31**, 55–138.
31 H. Dancygier, *Klinische Hepatologie Grundlagen, Diagnostik und Therapie hepatobiliärer Erkrankungen*, Springer-Verlag, Berlin Heidelberg New York, 2003.
32 Zakim, T. D. Boyer, M. P. Manns and A. J. Sanyal, *Hepatolog: A Textbook of Liver Disease*, Saunders Elsevier, Philadelphia, 2012.
33 F. Braet and E. Wisse, *Comp. Hepatol.*, 2002, **1**, 1.
34 K. Elvevold, B. Smedsrød and I. Martinez, *Am. J. Physiol.: Gastrointest. Liver Physiol.*, 2008, **294**, G391–400.
35 K. Jungermann, *Histochem. Cell Biol.*, 1995, **103**, 81–91.
36 G. Ramadori, *Virchow Arch. Pathol. Anat. Physiol. Klin. Med*, 1991, **61**, 147–158.
37 J. S. Lee, D. Semela, J. Iredale and V. H. Shah, *Hepatology*, 2007, **45**, 817–25.
38 L. Riccalton-Banks, C. Liew, R. Bhandari, J. Fry and K. Shakesheff, *Tissue Eng.*, 2003, **9**, 401–10.
39 S. L. Friedman, *Physiol. Rev.*, 2008, **88**, 125–172.
40 S. R. Khetani and S. N. Bhatia, *Nat. Biotechnol.*, 2008, **26**, 120–6.
41 C. Guguen-Guillouzo and A. Guillouzo, *General Review on In Vitro Hepatocyte Models and Their Applications*, Humana Press, Totowa, NJ, 2010, vol. 640.
42 G. Catapano and J. C. Gerlach, *Bioreactors for Liver Tissue*, 2007, vol. 3.
43 Y. Wang, T. Susando, X. Lei, C. Anene-Nzelu, H. Zhou, L. H. Liang and H. Yu, *Biointerphases*, 2010, **5**, FA116–31.
44 A. Dash, W. Inman, K. Hoffmaster, S. Sevidal, J. Kelly, R. S. Obach, L. G. Griffith and S. R. Tannenbaum, *Expert Opin. Drug Metab. Toxicol.*, 2009, **5**, 1159–74.
45 R. Gebhardt, J. G. Hengstler, D. Müller, R. Glöckner, P. Buenning, B. Laube, E. Schmelzer, M. Ullrich, D. Utesch, N. Hewitt, M. Ringel, B. R. Hilz, A. Bader, A. Langsch, T. Koose, H.-J. Burger, J. Maas and F. Oesch, *Drug Metab. Rev.*, 2003, **35**, 145–213.
46 K. Takahashi, K. Tanabe, M. Ohnuki, M. Narita, T. Ichisaka and K. Tomoda, *Cell*, 2007, **131**, 861–872.
47 K. Takahashi, K. Okita, M. Nakagawa and S. Yamanaka, *Nat. Protoc.*, 2007, **2**, 3081–3089.
48 H. Zhou, S. Wu, J. Y. Joo, S. Zhu, D. W. Han, T. Lin, S. Trauger, G. Bien, S. Yao, Y. Zhu, G. Siuzdak, H. R. Schöler, L. Duan and S. Ding, *Cell Stem Cell*, 2009, **4**, 381–4.
49 J. Yu, M. A. Vodyanik, K. Smuga-Otto, J. Antosiewicz-Bourget, J. L. Frane, S. Tian, J. Nie, G. A. Jonsdottir, V. Ruotti, R. Stewart, I. I. Slukvin and J. A. Thomson, *Science*, 2007, **318**, 1917–20.
50 S. F. Badylak, D. Taylor and K. Uygun, *Annu. Rev. Biomed. Eng.*, 2011, **13**, 27–53.
51 R. Jover, *Expert Opin. Drug Metab. Toxicol.*, 2006, **2**, 183–212.
52 Y. Imura, K. Sato and E. Yoshimura, *Anal. Chem.*, 2010, **82**, 9983–8.
53 Y. Imura, E. Yoshimura and K. Sato, *Anal. Sci.*, 2012, **28**, 197–9.
54 A. Sin, K. C. Chin, M. F. Jamil, Y. Kostov, G. Rao and M. L. Shuler, *Biotechnol. Prog.*, 2004, **20**, 338–45.
55 J. H. Sung and M. L. Shuler, *Lab Chip*, 2009, **9**, 1385–94.
56 M. L. Shuler, *Ann. Biomed. Eng.*, 2012, **40**, 1399–407.

57 R. Baudoin, L. Griscom, J. M. Prot, C. Legallais and E. Leclerc, *Biochem. Eng. J.*, 2011, **53**, 172–181.
58 J.-M. Prot, C. Aninat, L. Griscom, F. Razan, C. Brochot, C. G. Guillouzo, C. Legallais, A. Corlu and E. Leclerc, *Biotechnol. Bioeng.*, 2011, **108**, 1704–15.
59 M. A. Guzzardi, F. Vozzi and A. D. Ahluwalia, *Tissue Eng. A*, 2009, **15**, 3635–44.
60 F. Vozzi, D. Ph, J. Heinrich, A. Bader and A. D. Ahluwalia, *Tissue Eng. A*, 2009, **15**, 1291–1299.
61 B. Ma, G. Zhang, J. Qin and B. Lin, *Lab Chip*, 2009, **9**, 232–8.
62 Y.-C. Toh, C. Zhang, J. Zhang, Y. M. Khong, S. Chang, V. D. Samper, D. van Noort, D. W. Hutmacher and H. Yu, *Lab Chip*, 2007, **7**, 302–9.
63 C. Zhang, Z. Zhao, N. A. Abdul Rahim, D. van Noort and H. Yu, *Lab Chip*, 2009, **9**, 3185–92.
64 S.-M. Ong, C. Zhang, Y.-C. Toh, S. H. Kim, H. L. Foo, C. H. Tan, D. van Noort, S. Park and H. Yu, *Biomaterials*, 2008, **29**, 3237–44.
65 C. Zhang, S.-M. Chia, S.-M. Ong, S. Zhang, Y.-C. Toh, D. van Noort and H. Yu, *Biomaterials*, 2009, **30**, 3847–53.
66 V. N. Goral, Y.-C. Hsieh, O. N. Petzold, J. S. Clark, P. K. Yuen and R. A. Faris, *Lab Chip*, 2010, **10**, 3380–6.
67 M. Y. Zhang, P. J. Lee, P. J. Hung, T. Johnson, L. P. Lee and M. R. K. Mofrad, *Biomed. Microdevices*, 2008, **10**, 117–21.
68 P. J. Lee, P. J. Hung and L. P. Lee, *Biotechnol. Bioeng.*, 2007, **97**, 1340–1346.
69 R. Meissner, B. Eker, H. Kasi, A. Bertsch and P. Renaud, *Lab Chip*, 2011, **11**, 2352–61.
70 K. Domansky, W. Inman, J. Serdy, A. Dash, M. H. M. Lim and L. G. Griffith, *Lab Chip*, 2010, **10**, 51–8.
71 P. M. van Midwoud, G. M. M. Groothuis, M. T. Merema and E. Verpoorte, *Biotechnol. Bioeng.*, 2010, **105**, 184–94.
72 P. M. van Midwoud, M. T. Merema, N. Verweij, G. M. M. Groothuis and E. Verpoorte, *Biotechnol. Bioeng.*, 2011, **108**, 1404–12.
73 S. M. Hattersley, C. E. Dyer, J. Greenman and S. J. Haswell, *Lab Chip*, 2008, **8**, 1842–6.
74 M. J. Powers, K. Domansky, M. R. Kaazempur-Mofrad, A. Kalezi, A. Capitano, A. Upadhyaya, P. Kurzawski, K. E. Wack, D. B. Stolz, R. Kamm and L. G. Griffith, *Biotechnol. Bioeng.*, 2002, **78**, 257–269.
75 A. J. Hwa, R. C. Fry, A. Sivaraman, P. T. So, L. D. Samson, D. B. Stolz and L. G. Griffith, *FASEB J.*, 2007, **21**, 2564–79.
76 M. Powers, J. Janigian, K. E. Wack, C. E. Baker, D. B. Stolz and L. G. Griffith, *Tissue Eng.*, 2002, **8**, 499–513.
77 M. Lübberstedt, U. Müller-Vieira, M. Mayer, K. M. Biemel, F. Knöspel, D. Knobeloch, A. K. Nüssler, J. C. Gerlach and K. Zeilinger, *J. Pharmacol. Toxicol. Methods*, 2010, **63**, 59–68.
78 K. Zeilinger, T. Schreiter, M. Darnell, T. Söderdahl, M. Lübberstedt, B. Dillner, D. Knobeloch, A. K. Nüssler and J. C. Gerlach, *Tissue Eng., Part C*, 2011, 549–556.
79 M. A. Hamburg, *Science*, 2012, **336**, 299–300.
80 K. H. Liao, Y.-M. Tan and H. J. Clewell, *Risk Anal.*, 2007, **27**, 1223–36.
81 H. J. Clewell, J. M. Gearhart, P. R. Gentry, T. R. Covington, C. B. VanLandingham, K. S. Crump and A. M. Shipp, *Risk Anal.*, 1999, **19**, 547–58.
82 M. Dellian, G. Helmlinger, F. Yuan and R. K. Jain, *Br. J. Cancer*, 1996, **74**, 1206–15.
83 S. Khaustova, M. Shkurnikov, E. Tonevitsky, V. Artyushenko and A. Tonevitsky, *Analyst*, 2010, **135**, 3183–92.
84 D. A. Sakharov, D. V. Maltseva, E. A. Riabenko, M. U. Shkurnikov, H. Northoff, A. G. Tonevitsky and A. I. Grigoriev, *Eur. J. Appl. Physiol.*, 2012, **112**, 963–72.